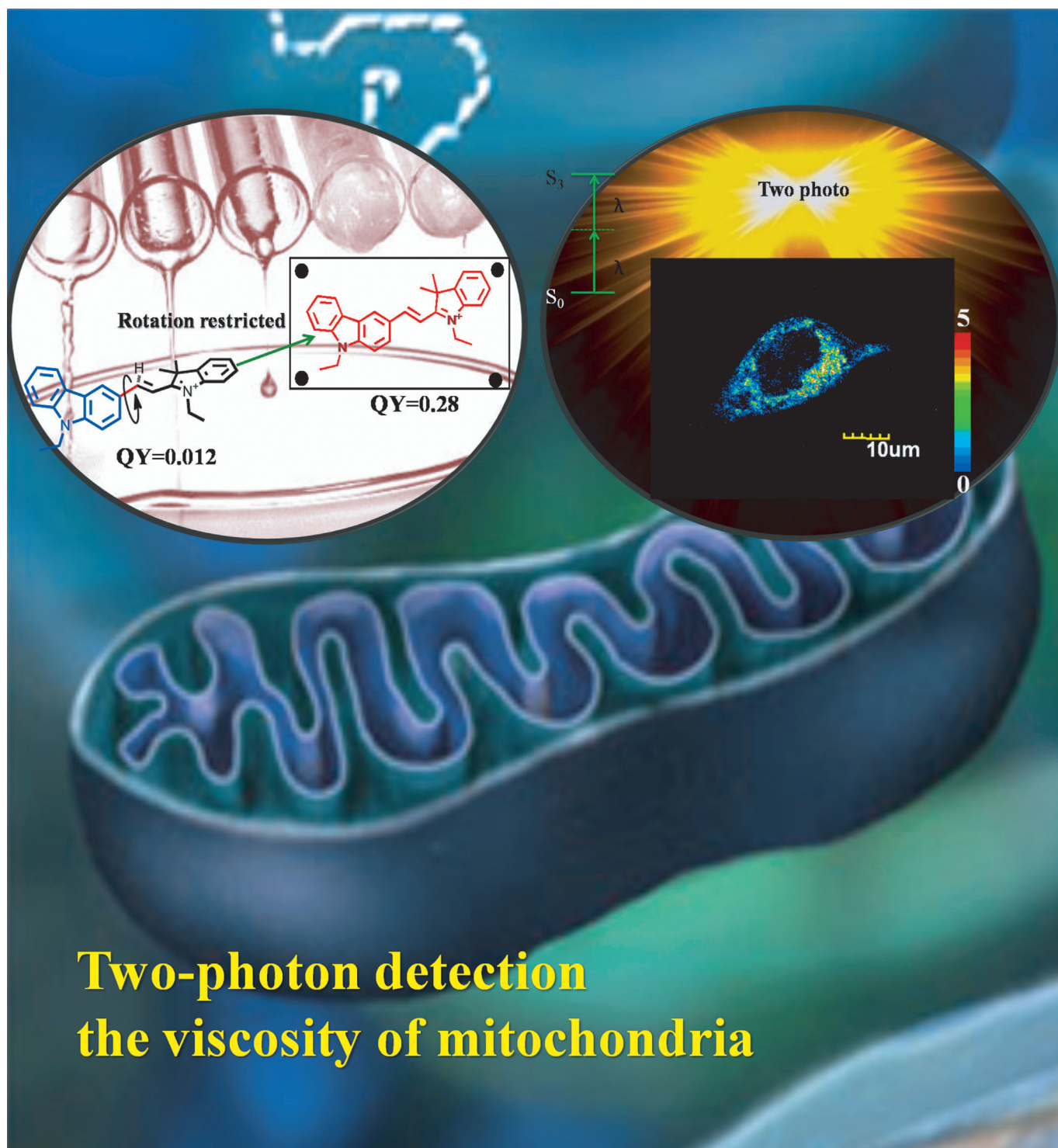


Ratiometric Detection of Viscosity Using a Two-Photon Fluorescent Sensor

Fei Liu,^[a] Tong Wu,^[a] Jianfang Cao,^[a] Shuang Cui,^[b] Zhigang Yang,^[a] Xinxin Qiang,^[a] Shiguo Sun,^[a] Fengling Song,^[a] Jiangli Fan,^[a] Jingyun Wang,^{*,[b]} and Xiaojun Peng^{*,[a]}



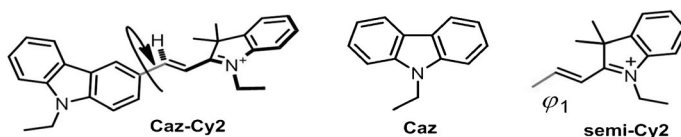
Cellular viscosity is known to influence how biomolecules and chemical signals interact and are transported within live cells, and consequently abnormal changes in cellular viscosity are related to cellular aspects of many diseases and malfunctions.^[1,2] At this time, however, the existing mechanical methods for the measurement of viscosity cannot be applied at the cellular level.

As the rotation of a molecular rotor is an efficient quenching pathway in nonviscous media, a fluorescent compound coupled with a rotor moiety can result in weak intrinsic fluorescence.^[3–8] However when the rotation is restricted, as in viscous media, emission is enhanced. Based on this principle, Theodorakis et al.^[9] produced a ratiometric viscosity sensor comprising a dye with two distinct fluorescent units. A coumarin acted as a donor fluorophore to induce excitation of the rotor moiety (CMAM) by means of resonance energy transfer (RET), thereby allowing rapid measurement of the viscosity. Suhling et al.^[10] reported a dipyrin fluorescent sensor in which restricted rotation of a phenyl group permitted the imaging of the local microviscosity. Our group subsequently reported a fluorescent sensor **RY3**, in which an aldehyde group (–CH=O) acted as a rotor to measure the intracellular viscosity.^[11] **RY3** was the first molecular rotor capable of dual-mode fluorescence imaging, potentially permitting investigation of the pathologies of diseases.

Recently, two-photon microscopy (TPM), which employs two near-infrared photons as the excitation source, has become important in bioimaging applications.^[12,13] Thus, TPM has the advantage of offering intrinsic 3D resolution combined with reduced phototoxicity, increased specimen penetration (> 500 μm), localized excitation, and prolonged observation time.^[14–17] In addition, the long-wavelength excitation (> 700 nm) effectively avoids background interference owing to the autofluorescence of the biomatrix. Recently, Cho's^[18,19] group developed a series of two-photon fluorescent sensors based on the naphthalene framework that can be used in live cells and intact tissues and is visualized by TPM. However, although the TPM technique and TPM sensors have been applied in the detection of metal ions and small molecules, and for the labeling of proteins and DNA, to our knowledge, no TPM sensor has yet been found that detects cellular microenvironmental viscosity, especially in

living tissues. In the fields of biological research and pathology, using the TPM technique and chemicals to visualize viscosity are very significant.

In the present investigation, a carbazole-based cyanine derivative **Caz-Cy2** ($\lambda_{\text{abs}}=485\text{ nm}$; $\lambda_{\text{em}}(\text{blue})=380\text{ nm}$,



$\lambda_{\text{em}}(\text{red})=580\text{ nm}$) was synthesized by linking the **Caz** and **semi-Cy2** moieties to give rise to a ratiometric two-photon (TP) viscosity sensor. The spectrum of **Caz** has a short wavelength peak similar to **Caz-Cy2** ($\lambda_{\text{abs}}=345\text{ nm}$, $\lambda_{\text{em}}(\text{blue})=368\text{ nm}$; Figures S1 and S2 in the Supporting Information). **Semi-Cy2**, the conjugated electron acceptor, was hypothesized to be rotated around bond φ_1 (labeled red in the formulae) with **Caz** in unconstrained environments, and so gave rise to the red emission. Compared with traditional cyanine dyes such as **Cy3** and **Cy5**, **Caz-Cy2** showed unique spectroscopic characteristics, such as very low fluorescence in nonviscous solvents and a large Stokes shift (> 100 nm). As shown in Figure 1, the quantum yield (QY) of **Caz-Cy2**

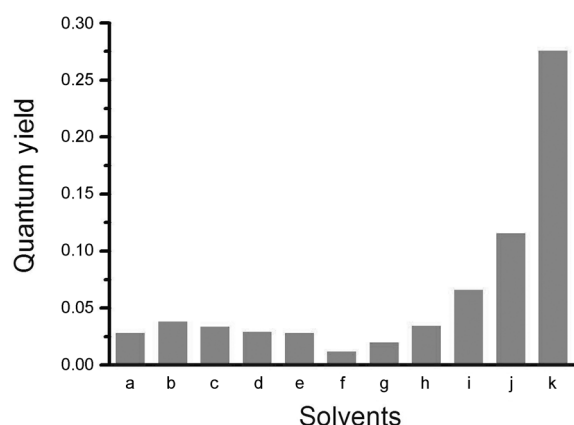


Figure 1. A histogram showing the fluorescence quantum yields of **Caz-Cy2** ($1\ \mu\text{M}$) in different solvents ($\lambda_{\text{em}}=580\text{ nm}$): a) dichloromethane, b) DMSO, c) ethanol, d) dioxane, e) methanol, f) water, g) water/glycerol (8:2 v/v), h) water/glycerol (6:4 v/v), i) water/glycerol (4:6 v/v), j) water/glycerol (2:8 v/v), k) glycerol (99%). Rhodamine B was used as a standard reference with a fluorescence quantum yield of 0.97 in ethanol.

was very low, approximately 0.012–0.04, in low-viscosity solvents, and was not apparently affected by solvent polarity. This is crucial to permit a molecular rotor to sense environmental viscosity.^[20] On the other hand, **Caz-Cy2** showed a dramatic fluorescence enhancement with increases of the solvent viscosity. As glycerol was gradually added to water, the viscosity of the solutions increased from 1.0 cP (water) to approximately 950 cP (99% glycerol), and paralleling this, the fluorescence of **Caz-Cy2** increased 23-fold (QY = 0.28) in 99% glycerol (Figure 1g–k).

[a] F. Liu, Dr. T. Wu, J. Cao, Dr. Z. Yang, Dr. X. Qiang, Dr. S. Sun, Dr. F. Song, Dr. J. Fan, Prof. X. Peng
State Key Laboratory of Fine Chemicals
Dalian University of Technology
No. 2 Linggong Road, High-Tech District
Dalian 116024 (P.R. China)
Fax: (+86) 411-84986306
E-mail: pengxj@dlut.edu.cn

[b] S. Cui, J. Wang
School of Life Science and Biotechnology
Dalian University of Technology
No. 2 Linggong Road, High-Tech District
Dalian 116024 (P.R. China)
E-mail: wangjingyun67@126.com

Supporting information for this article is available on the WWW under <http://dx.doi.org/10.1002/chem.201202646>.

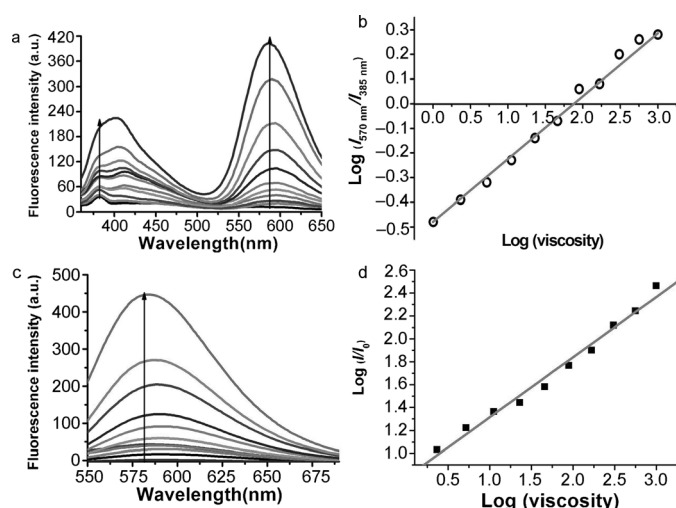


Figure 2. a) Changes in the fluorescence emission spectra of **Caz-Cy2** as a function of the solvent viscosity (excited at 335 nm); b) the linear response between the $\log(I_{580\text{nm}}/I_{385\text{nm}})$ and the $\log(\text{viscosity})$ in the water/glycerol solvent (excited at 335 nm); c) the red-fluorescence-emission spectra of **Caz-Cy2** as a function of solvent viscosity (excited at 480 nm); d) the linear response between $\log(I/I_0)$ and $\log(\text{viscosity})$ in the water/glycerol solvent (excited at 480 nm).

As illustrated in Figure 2, the fluorescence spectrum of **Caz-Cy2** possesses two emission bands in aqueous solution. The red-emission band ($\lambda_{\text{em}}(\text{red}) = 580 \text{ nm}$) of **Caz-Cy2** rose much faster than the blue-emission band ($\lambda_{\text{em}}(\text{blue}) = 380 \text{ nm}$) as the solvent viscosity was increased. Moreover, the logarithm of the fluorescence ratio thereof ($I_{580\text{nm}}/I_{380\text{nm}}$) had a linear relationship with that of the viscosity (η) of the solution, which was identical to that measured for the TP process (see Figure S3 in the Supporting Information). This is as expected from the Förster–Hoffmann equation [Eq. (1)]:^[21]

$$\log I_f = C + x \log \eta \quad (1)$$

in which C is a concentration- and temperature-dependent constant and x is a dye-dependent constant. Therefore, $\log(I_{580\text{nm}}/I_{385\text{nm}})$ of **Caz-Cy2** and $\log \eta$ were fitted accordingly. The R^2 of 0.99 and the slope x of 0.27 indicate that **Caz-Cy2** could be applied as a ratiometric sensor to quantitatively detect the solution viscosity (Figure 2b).

As shown in Figure 2c and d, we investigated the red-emission spectra of **Caz-Cy2** in mixtures of water and glycerol. The emission of rotor **Caz-Cy2** was greatly enhanced and exhibited a stable spectrum in its fluorescence intensity within one hour (Figure S5a in the Supporting Information) in solvents of high viscosity when excited at 480 nm. The emission intensity at 580 nm in glycerol was 80-fold that seen in water, and the logarithm of the fluorescence ratio thereof (I/I_0) at 580 nm showed a good linear relationship with that of the viscosity of the solution. The R^2 of 0.98 and the slope x of 0.52 indicate that **Caz-Cy2** could be applied with the fluorescence-enhancement method that senses the viscosity change by the rotor **Caz-Cy2**.

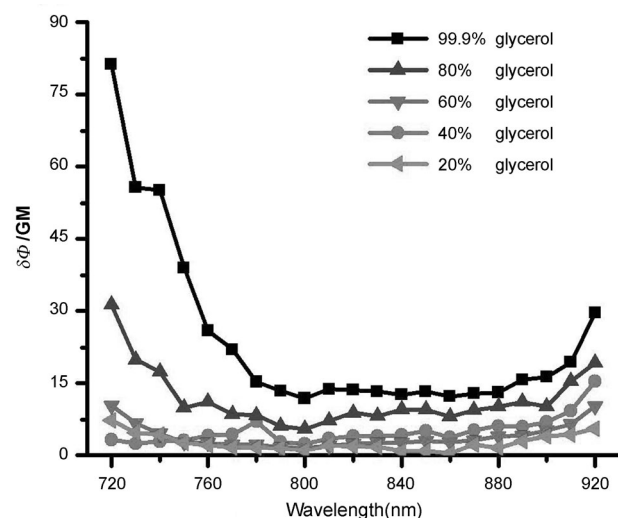


Figure 3. Two-photon (TP) action spectra of **Caz-Cy2** in solvents of varying viscosity. TP excitation: 720–920 nm.

Carbazole and its derivatives have been reported to have excellent two-photon properties.^[22–24] As shown in Figure 3, the two-photon absorption spectra of **Caz-Cy2** increased dramatically with a rise in solvent viscosity, which was achieved by increasing the proportion of glycerol in the water. From 1.0 P (water) to approximately 950 cP (99% glycerol), the two-photon action cross-section ($\delta\Phi$) at 720 and 920 nm increased from 3.9 to 81.2 GM and 5.3 to 29.6 GM, respectively (Figure 3; 1 GM = $10^{-50} \text{ cm}^4 \text{ s photon}^{-1}$).

Possible effects of intracellular biochemicals on the use of **Caz-Cy2** as a viscosity sensor were evaluated by adding various compounds to **Caz-Cy2** solutions. As seen in Figures S6 and S7 in the Supporting Information, the spectrum of the dye was influenced more by viscosity than by these biological species.

Cell-staining experiments showed that **Caz-Cy2** could readily enter live HeLa cells and give clear fluorescence images. To investigate the localization of **Caz-Cy2**, dual staining with two commercially available organelle sensors was carried out. As seen in Figure 4, the dye colocalized with the commercially available mitochondrial sensor, Mito Tracker Deep Red FM, with weighted colocalization coefficient values to 0.98 (analyzed using Olympus Micro FV10-ASW software). Dual staining of **Caz-Cy2** with the nuclear

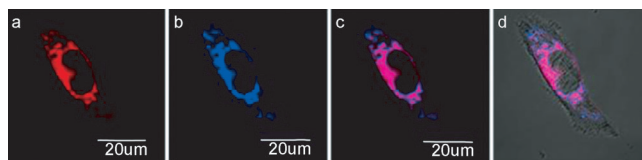


Figure 4. Live-cell counterstain of **Caz-Cy2** with MitoTracker Deep Red FM (MitoTracker for short). One- and two-photon excitation were at 488 and 720 nm, respectively: a) TPM image of **Caz-Cy2** (530–580 nm); b) OPM image of MitoTracker (690–740 nm); c) overlap of (a) and (b); d) overlap of (c) with the white-light image.

dye DRAQ 5, however, showed no colocalization (see Figure S8 in the Supporting Information).

A wide range of human diseases, such as cancers, Alzheimer's disease (AD), and diabetes, are closely related to mitochondrial dysfunction, which is caused by pathological processes, such as overproduction of reactive oxygen species (ROS), reactive nitrogen species (RNS), and amyloid beta peptide (A β).^[25–27] Such pathological processes may involve changes in viscosity, and consequently **Caz-Cy2** may offer a new approach to investigating such processes.

Since the fluorescence signal ratio is independent of the dye concentration or intracellular distribution, it is considered superior to using the intensity signal. So **Caz-Cy2** with two emission peaks can be also applied to the ratiometric fluorescence imaging of viscosity in live cells. Excited at 720 nm, the fluorescence images were obtained by collecting the blue emission of (375–440 nm) (green channel: Figure 5a) and the red emission of (575–645 nm) (red channel:

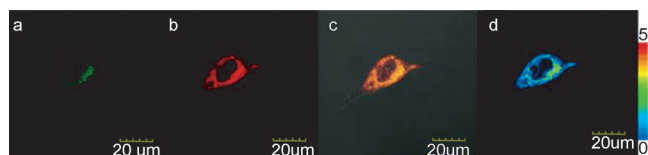


Figure 5. Live HeLa cell staining with **Caz-Cy2** (10 μM , 40 min incubation) excited at 720 nm. A 1000 \times magnification was utilized in the imaging: a) blue channel (375–440 nm); b) red channel (575–640 nm); c) overlap of images (a) and (b); d) the ratio image of **Caz-Cy2** obtained by the Image Pro-plus software.

Figure 5b). The ratio image ($I_{580\text{ nm}}/I_{380\text{ nm}}$) clearly displayed the distribution of viscosity in the cells. In Figure 5d, the “blue” imaging areas of HeLa cells indicate low viscosity with small ratio values (< 100 cP); the “green” regions indicate an intermediate viscosity with the ratio value of 100–500 cP; and the small intracellular red zones represent high viscosity microenvironments (> 900 cP) in cells.

We further investigated the application of this sensor in tissue imaging (Figure 6). A fresh rat hepar slice, incubated with 100 μM **Caz-Cy2** for 40 min, shows the viscosity distribution at a 110 μm depth. In Figure 6d, the “blue” imaging areas of the tissue slice indicate low viscosity with small ratio values (< 100 cP); the “green” regions indicate an intermediate viscosity with the ratio value of 100–500 cP; and

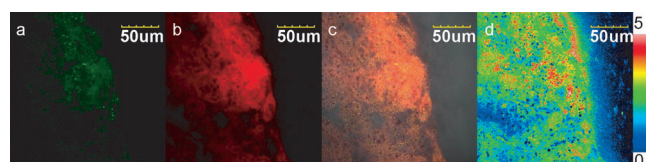


Figure 6. Images of a fresh rat hepar slice stained with **Caz-Cy2** (100 μM , 40 min incubation) at 110 μm depth, excited at 720 nm: a) blue channel (375–440 nm); b) red channel (575–640 nm); c) overlap of images (a), (b), and the white-light image; d) the ratio image of **Caz-Cy2** obtained by the Image Pro-plus software.

the small intracellular red zones represent high viscosity microenvironments (> 900 cP) in cells. It is worth noting that the changes in the emission ratios measured deep inside the tissue slice are comparable to those in the cells. Furthermore, it demonstrates that **Caz-Cy2** is capable of detecting viscosity at depths of 60–130 μm in live tissues using TPM (see Figure S9 in the Supporting Information). In addition, the two-photon excitation fluorescence (TPEF) stability of **Caz-Cy2** could be visualized for more than 44 min without appreciable decay in the tissue (see Figure S5b in the Supporting Information); this means that **Caz-Cy2** has a high photostability for deep-tissue imaging.

To clearly understand the rotor mechanism occurring with **Caz-Cy2**, the molecular geometries and photophysical properties of **Caz-Cy2** were investigated computationally (see the Supporting Information). A DFT study of **Caz-Cy2** confirmed that the nonradiative deactivation is mainly accessed by rotating the monomethine bridge. When this free rotation is restricted, it leads to an increase in the fluorescence quantum yield. As shown in Figure 7a, there are several methine bonds in **Caz-Cy2** that may be involved in the rotation. However, the results of the quantum chemical calculations were able to explain which of these caused the mainly nonradiative deactivation (see Figure S11 in the Supporting Information). The calculated activation energy and energy gap (the energy difference between the initial and final electron-

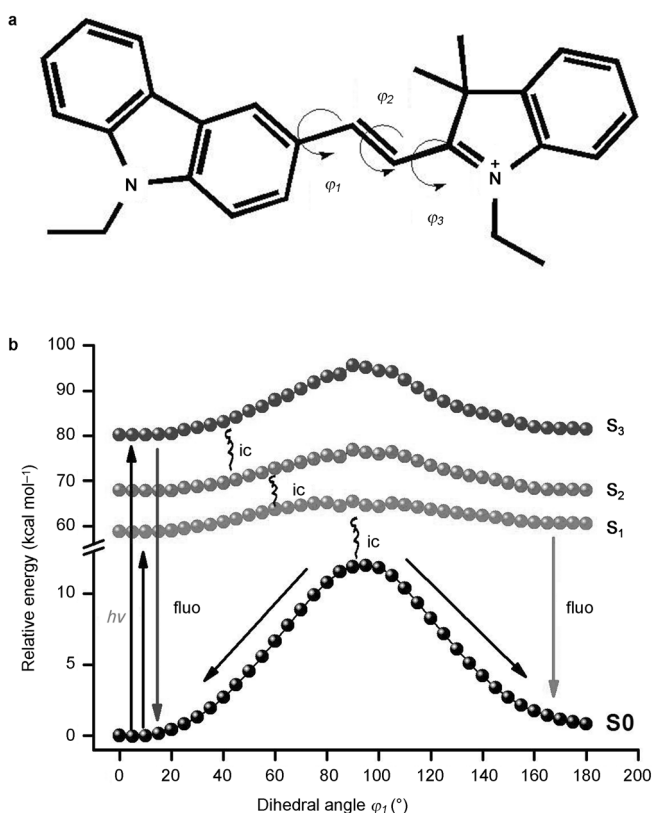


Figure 7. a) The probable rotation of different chemical bonds. b) Potential-energy curves of **Caz-Cy2** at the energy levels of the S_0 , S_1 , S_2 , and S_3 states with torsion angles around bond φ_1 ; ic = intersystem crossing.

ic states) for rotations around different chemical bonds in **Caz-Cy2** in the S_0 and S_1 states are listed in Table S1 in the Supporting Information. The data suggest that rotation about the central double bond (φ_2) is most difficult, since there is a higher energy barrier to rotation in the S_1 state. The rotation around the indolium–ethylene bond (φ_3) is also impossible, since there is a large energy gap to the ground state, and the decay rate of excited electronic states depends exponentially on the energy gap. The state formed by twisting of the φ_1 bond possesses a remarkably low energy gap to the ground state, and a lower barrier to rotation in the S_1 state, which causes mainly nonradiative deactivation (Figure 7b).

In conclusion, a carbazole-based cyanine derivative **Caz-Cy2** ($\lambda_{\text{abs}} = 485$ nm; $\lambda_{\text{em}}(\text{blue}) = 380$ nm, $\lambda_{\text{em}}(\text{red}) = 580$ nm) was developed as a ratiometric TP viscosity sensor. **Caz-Cy2** was able to quantitatively detect the solution viscosity without any apparent influence from the environmental polarity or biomacromolecules. **Caz-Cy2** is an excellent TP rotor sensor candidate that appears able to report on the viscosity of mitochondria in live cells as well as in living tissues at depths of 60–130 μm by ratiometric fluorescence imaging.

Experimental Section

Viscosity determination and fluorescence spectral measurement detection: The solvents were obtained by mixing a water/glycerol system. Measurements were carried out with a NDJ-7 rotational viscometer, and each viscosity value was recorded. The solutions of **Caz-Cy2** of different viscosity were prepared by adding the stock solution (1.0 mM) to the solvent mixture (10 mL; water/glycerol) to obtain the final concentration of the dye (1.0 μM). These solutions were sonicated for 5 min to eliminate air bubbles. After standing for 1 h at a constant temperature, the solutions were measured in a UV spectrophotometer and a fluorescence spectrophotometer.

Absorption and fluorescence-quantum-yield measurements: Absorption spectra were measured on a Lamda LS35 spectrophotometer. Fluorescence spectra were obtained with a FP-6500 spectrophotometer (Jasco, Japan). The relative fluorescence quantum yields were determined with rhodamine B as a standard and were calculated using Equation (2):

$$\Phi_x = \Phi_s(F_x/F_s)(A_s/A_x)(\lambda_{\text{exs}}/\lambda_{\text{exx}})(n_x/n_s)^2$$

in which Φ represents the quantum yield, F stands for the integrated area under the corrected emission spectrum, A is the absorbance at the excitation wavelength, λ_{ex} is the excitation wavelength, n is the refractive index of the solution (because of the low concentrations of the solutions (10^{-7} – 10^{-8} molL $^{-1}$), the refractive indices of the solutions were replaced with those of the solvents), and the subscripts x and s refer to the unknown and the standard, respectively.

Measurement of the TP cross-section: The TP cross-section (δ) was determined by using a femtosecond (fs) fluorescence measurement technique as described in the literature.^[28] The TP-induced fluorescence intensity was measured at 720–900 nm by using rhodamine 6G as the reference, the two-photon property of which has been well characterized in the literature.^[29] The intensities of the two-photon-induced fluorescence spectra of the reference and sample emitted at the same excitation wavelength were determined. The TPA cross-section was calculated by using Equation (3):

$$\delta = \delta_r(S_s\Phi_r\phi_r c_r)/(S_r\Phi_s\phi_s c_s)$$

in which the subscripts s and r stand for the sample and reference molecules, respectively. The intensity of the signal collected by a charged-coupled device (CCD) detector was denoted as S . Φ is the fluorescence quantum yield. ϕ is the overall fluorescence collection efficiency of the experimental apparatus. The number density of the molecules in solution was denoted as c . δ_r is the TPA cross-section of the reference molecule.

Live-cell incubation: HeLa cells were cultured in Dulbecco's modified Eagle's medium (DMEM; Invitrogen) supplemented with 10% fetal calf serum (FCS; Invitrogen). One day before imaging, the cells were seeded into 24-well flat-bottomed plates. The next day, the cells were incubated with 8.0 μM dye for 40 min at 37°C under 5% CO $_2$ and washed with phosphate-buffered saline (PBS) three times.

Preparation and staining of the tumor slices: Tumor slices were prepared from nude mice, which were seeded S180 cells. Normal tissue slices were prepared from the liver of nude mice. Slices were incubated with **Caz-Cy2** (20 μM) in artificial cerebrospinal fluid (ACSF; 138.6 mM NaCl, 3.5 mM KCl, 21 mM NaHCO $_3$, 0.6 mM NaH $_2$ PO $_4$, 9.9 mM D-glucose, 1 mM CaCl $_2$, and 3 mM MgCl $_2$) bubbled with 95% O $_2$ and 5% CO $_2$ for 30 min at 37°C. Slices were then washed three times with ACSF and transferred to a glass-bottomed dish (MatTek, 35 mm dish with 20 mm bottom well) and observed in a spectral confocal multiphoton microscope.

Fluorescence imaging: One-photon fluorescence imaging and two-photon fluorescence ratio imaging of **Caz-Cy2** in cells were obtained with spectral confocal multiphoton microscopes (Leica TCS SP2). Two-photon fluorescence microscopy images of **Caz-Cy2** and cells were obtained with a DM IRE2 microscope (Leica) by exciting **Caz-Cy2** with a mode-locked titanium–sapphire laser source (Coherent Chameleon, 90 MHz, 200 fs) set at a wavelength of 720 nm and output power of 1230 mW.

The photostability test: The two-photon photostability of **Caz-Cy2** was established as described in the literature.^[30] A microscope was used and **Caz-Cy2** was excited with a mode-locked titanium–sapphire laser source (Coherent Chameleon, 90 MHz, 200 fs) set at a wavelength of 720 nm and an output power of 1230 mW, which corresponded to an approximately 10 mW average power in the focal plane. In this process, the laser has been turned on and is continuously exciting the sample. A CCD recorded a set of intensities at various time intervals (2 min) during 44 min. Moreover, the average intensity of every set of intensities data was calculated by using Olympus Fluoview, version 3.0, software.

Synthesis of Caz-Cy2: Quaternized salt **c** (1.58 g, 5.0 mmol) and aldehyde **b** (1.00 g, 4.5 mmol) were added to a 100 mL flask with ethanol (50 mL), followed by piperidine catalyst (1.0 mL). The mixture was stirred for 12 h at 80°C. On standing at room temperature, a residue precipitated out from ethanol; further recrystallization in ethanol gave the desired product. M.p. 120–122°C; $^1\text{H NMR}$ (400 MHz, CDCl $_3$): $\delta = 9.11$ – 9.05 (m, 1H), 8.54 (s, 1H), 8.47 (d, $J = 8.7$ Hz, 1H), 8.41 (d, $J = 15.8$ Hz, 1H), 7.91 (d, $J = 15.8$ Hz, 1H), 7.52 (d, $J = 12.6$ Hz, 5H), 7.42 (s, 2H), 7.33 (s, 1H), 5.01 (d, $J = 7.3$ Hz, 2H), 4.32 (d, $J = 7.2$ Hz, 2H), 1.85 (s, 6H), 1.62 (s, 3H), 1.43 ppm (t, $J = 7.2$ Hz, 3H); $^{13}\text{C NMR}$ (101 MHz, CDCl $_3$): $\delta = 157.27$, 144.20, 140.45, 130.79, 129.43, 128.70, 127.02, 125.43, 124.39, 121.14, 113.95, 108.80, 77.78, 77.05, 76.73, 38.16, 27.68 ppm; HR-TOF-MS: m/z calcd for C $_{28}$ H $_{29}$ N $_2^+$ [M] $^+$: 393.2325; found: 393.2338.

Acknowledgements

This work was supported by the National Science Foundation of China (21136002, 21076032, 20923006), the National Basic Research Program of China (2009CB724706, 2013CB733702), the High Technology Research and Development Program of China (863 program) (2011AA02A105).

Keywords: cells • fluorescence • sensors • two-photon microscopy • viscosity

- [1] M. J. Stutts, C. M. Canessa, J. C. Olsen, M. Hamrick, J. A. Cohn, B. C. Rossier, R. C. Boucher, *Science* **1995**, *269*, 847–850.
- [2] K. Luby-Phelps, *Int. Rev. Cytol.* **1999**, *192*, 189–221.
- [3] M. A. Haidekker, E. A. Theodorakis, *Org. Biomol. Chem.* **2007**, *5*, 1669–1678.
- [4] D. E. Fischer, A. Theodorakis, M. A. Haidekker, *Nat. Protoc.* **2007**, *2*, 227–236.
- [5] M. K. Kuimova, G. Yahioglu, J. A. Levitt, K. Suhling, *J. Am. Chem. Soc.* **2008**, *130*, 6672–6673.
- [6] M. K. Kuimova, S. W. Botchway, A. W. Parker, M. Balaz, H. A. Collins, H. L. Anderson, K. Suhling, P. R. Ogilby, *Nat. Chem.* **2009**, *1*, 69–73.
- [7] J. Shao, S. Ji, X. Li, J. Zhao, F. Zhou, H. Guo, *Eur. J. Org. Chem.* **2011**, 6100–6109.
- [8] F. Zhou, J. Shao, Y. Yang, J. Zhao, H. Guo, X. Li, J. Shao, Z. Zhang, *Eur. J. Org. Chem.* **2011**, 4773–4787.
- [9] M. A. Haidekker, T. P. Brady, D. Lichlyter, E. A. Theodorakis, *J. Am. Chem. Soc.* **2006**, *128*, 398–399.
- [10] K. Suhling, P. M. French, D. Phillips, *Photochem. Photobiol. Sci.* **2005**, *4*, 13–22.
- [11] X. Peng, Z. Yang, J. Wang, J. Fan, Y. He, F. Song, B. Wang, S. Sun, J. Qu, J. Qi, M. Yan, *J. Am. Chem. Soc.* **2011**, *133*, 6626–6635.
- [12] J. A. Feijó, N. Moreno, *Protoplasma* **2004**, *223*, 1–32.
- [13] H. M. Kim, B. R. Cho, *Acc. Chem. Res.* **2009**, *42*, 863–872.
- [14] F. Helmchen, W. Denk, *Nat. Methods* **2005**, *2*, 932–940.
- [15] W. R. Zipfel, R. M. Williams, W. W. Webb, *Nat. Biotechnol.* **2003**, *21*, 1369.
- [16] W. Denk, J. Strickler, W. W. Webb, *Science* **1990**, *248*, 73–76.
- [17] P. T. So, C. Y. Dong, B. R. Masters, K. M. Berland, *Annu. Rev. Biomed. Eng.* **2000**, *2*, 399–429.
- [18] C. S. Lim, G. Masanta, H. J. Kim, J. Han, M. Kim, B. R. Cho, *J. Am. Chem. Soc.* **2011**, *133*, 11132–11135.
- [19] G. Masanta, C. S. Lim, H. J. Kim, J. H. Han, H. M. Kim, B. R. Cho, *J. Am. Chem. Soc.* **2011**, *133*, 5698–5700.
- [20] M. A. Haidekker, T. P. Brady, D. Lichlyter, E. A. Theodorakis, *Bioorg. Chem.* **2005**, *33*, 415–425.
- [21] Th. Förster, G. Z. Hoffmann, *Z. Phys. Chem.* **1971**, *75*, 63–76.
- [22] X. Liu, Y. Sun, Y. Zhang, F. Miao, G. Wang, H. Zhao, X. Yu, H. Liu, W. Wong, *Org. Biomol. Chem.* **2011**, *9*, 3615–3618.
- [23] X. J. Feng, P. L. Wu, F. Bolze, H. W. Leung, K. F. Li, N. K. Mak, D. W. Kwong, J. F. Nicoud, K. W. Cheah, M. S. Wong, *Org. Lett.* **2010**, *12*, 2194–2197.
- [24] J. Gu, Y. Wang, W. Chen, X. Dong, X. Duan, S. Kawata, *New J. Chem.* **2007**, *31*, 63–68.
- [25] A. M. Aleardi, G. Benard, O. Augereau, M. Malgat, J. C. Talbot, J. P. Mazat, T. Letellier, J. Dachary-Prigent, G. C. Solaini, Rossignol, *J. Bioenerg. Biomembr.* **2005**, *37*, 207–225.
- [26] A. I. García-Peréz, E. A. López-Beltrán, P. Klüner, J. Luque, P. Bal- lesteros, S. Cerdán, *Arch. Biochem. Biophys.* **1999**, *362*, 329–338.
- [27] W. Junge, *FEBS Lett.* **1972**, *25*, 109–112.
- [28] S. K. Lee, W. J. Yang, J. J. Choi, C. H. Kim, S. J. Jeon, B. R. Cho, *Org. Lett.* **2005**, *7*, 323–326.
- [29] N. S. Makarov, M. Drobizhev, A. Rebane, *Optics Express.* **2008**, *6*, 4029–4047.
- [30] H. Kim, W. Yang, C. Kim, W. Park, S. Jeon, B. Cho, *Chem. Eur. J.* **2005**, *11*, 6386–6391.

Received: July 25, 2012

Revised: November 12, 2012

Published online: December 19, 2012